geosciences

MDPI

Article

Characterization of Gold of the Murcielago Fluvial Placer (Central Honduras) and Its Possible Primary Sources

Sabrina Nazzareni [1,*,†], Simona Alunno [2,†,‡], Federica Zaccarini [3,†], Michele Mattioli [4,†], Alessandro Murroni [5,†], Alessandro Di Michele [1,†] and Alberto Renzulli [4,†]

1 Dipartimento di Fisica e Geologia, Università di Perugia, 06123 Perugia, Italy; alessandro.dimichele@unipg.it
2 Goldlake Group, 05024 Gubbio, Italy
3 Geosciences Programme, Faculty of Science, University Brunei Darussalam, Jalan Tungku Link, Gadong, Bandar Seri Begawan BE1410, Brunei
4 Dipartimento di Scienze Pure e Applicate, University of Urbino Carlo Bo, 61029 Urbino, Italy
5 Loc. S'Arriali, 09016 Iglesias, Italy
* Correspondence: sabrina.nazzareni@unipg.it
† These authors contributed equally to this work.
‡ Current address: via Galeotti 36, 06024 Gubbio, Italy.

Abstract: The Murcielago gold placer is located in the Lepaguare Valley, Olancho Department (Central Honduras). The placer mineralogy includes silicates (quartz, garnets, amphibole, Ca-pyroxene, micas, epidote, and tourmaline); calcite; and in the heavy fraction, zircon, ilmenite–rutile, magnetite, hematite, cassiterite, and cinnabar. Gold grains recovered from the Murcielago placer production plant are mainly flattened grains with a moderately to high elliptical shape. The composition of the gold grains varies continuously in the range $Au_{46}Ag_{54}$ to $Au_{88}Ag_{12}$. Few of them are characterized by Au-rich rims of a few microns in size (Ag 3-1 atoms percent (at%)). Gold from the Canan lode deposit, a nearby hydrothermal Au mineralization area, has a composition (from $Au_{54}Ag_{44}$ to $Au_{81}Ag_{19}$) overlapping the composition of the Murcielago grains. Inclusions in the alluvial gold particles are arsenopyrite, pyrite, acanthite, sphalerite, and hematite. On the basis of the placer mineralogy and the gold grains analyses, possible gold source(s) include the Canan lode and skarn gold deposits in the area. We obtained new data on the Murcielago gold placer that will be the basis for an exploration of the potential sources of gold in the area.

Keywords: gold grains; electron microprobe; gold deposit; placer; lode gold; Central America; Honduras; minerals; geochemistry

Citation: Nazzareni, S.; Alunno, S.; Zaccarini, F.; Mattioli, M.; Murroni, A.; Michele, A.D.; Renzulli, A. Characterization of Gold of the Murcielago Fluvial Placer (Central Honduras) and Its Possible Primary Sources. *Geosciences* **2023**, *13*, 175. https://doi.org/10.3390/geosciences13060175

Academic Editors: Paul Alexandre and Jesus Martinez-Frias

Received: 12 March 2023
Revised: 3 June 2023
Accepted: 6 June 2023
Published: 10 June 2023

1. Introduction

Gold deposits are widespread in Central America and the Caribbean area (e.g., [1–6]), both as lode or placer deposits. Despite the strong interest in gold exploitation, the knowledge on the origin of this type of mineralization and mineralogical data are still insufficient for several Central American areas, Honduras included (e.g., [3,7–14]. Honduras gold deposits, as reported by Nelson [3,15,16], are epithermal, skarn, and orogenic types. The epithermal Au deposit type is the most widespread with respect to skarn and orogenic Au deposit types. Gold mineralization occurs as high-grade veins and breccia pipes (Bonanza veins) or as stockwork and disseminated (fossil hot spring system) in epithermal deposits, some of which have potential exploitation interest (San Andres with current resource 20.5 Mt at 1.1 g/t Au, Rosa with current resource 34.9 Mt at 0.86 g/t Au, Yuscaran with current resource 0.5 Mt at 5.0 g/t) [3]. Skarn deposit mineralizations are Cu–Au–Mo ore bodies related to the Paleozoic igneous activity that intruded in the Mesozoic carbonates and redbed sediments. The most known mineralization is the Minas de Oro area that was exploited during historical times, Minas Viejas having current resources of 2.2 Mt at 0.8 g/t Au, Montecielo with 3.3 Mt at 0.9 g/t Au, and Tatanacho with 6.2 Mt at 0.7 g/t Au. Two

other areas are Opoteca (with current resources of 1.3 Mt at 0.17 g/t Au) and Mochito (with current resources 3.4 Mt at 78g/t Au) [3]. Skarn has the typical carbonate-hosted skarn mineralogy with garnet, clinopyroxene, and epidote associated with magnetite and massive sulfide (pyrite, chalcopyrite, sphalerite, and galena) and quartz, calcite, and chlorite as gangue minerals. Orogenic gold deposits are located mainly in the NW (Vueltas del Rio, Chapareles and Zopilote Jocotan fault) and minorly in the SE part of the country. These deposits are mainly hosted in a sequence of marine siltstone, basalt flow, volcaniclastic rocks, and limestone in the Montagua suture zone (a left strike-slip fault system related to the westward drift of the North American plate with respect to the Carribean plate) [15]. Although secondary placer deposits are known, a systematic study on the geochemical characterization and origin of the alluvial gold is absent. The Murcielago gold placer is located in the Olancho Department (Honduras) and has been exploited since 2004 by Eurocantera (a subsidiary of the Goldlake Group). In the area, epithermal and skarn gold deposits are reported, but the alluvial gold source is unknown. Moreover the Murcielago gold placer mine is a pilot example of green and sustainable extraction developed by an ecofriendly technology (Appendix A). Here the gold exploitation is only based on gravimetric separation without grinding steps or any use of cyanide or harmful chemicals.

In this paper, we present a chemical characterization of the gold grains from the Murcielago placer and Canan's nearby lode deposit. Moreover we have analyzed the morphology of the Murcielago gold grains to add information about the transport and possible source(s). In a placer environment, gold grains may form by purely accretionary detrital mechanisms, but supergene processes may also play an important role [17]. Attempts to link the morphology and chemistry of alluvial gold to process and origin have been done (e.g., [18–21]). Morphology has been proved to be an index of transport but rarely of origin. By contrast, chemistry can be used to infer origin and processes. Grain morphology is influenced by numerous factors, including the character of the original lode particles, stream energy, nature of the stream channel material, time spent in the stream, distance of transport, and chemistry of the stream water. Grain morphology during alluvial transport evolves in a predictable trend from the original irregular form through to semispherical and wafer-like, ultimately yielding flake shapes [20].

The placer mineralogy was also characterized to have information about the possible gold source(s). As far as we know, these are the first chemical data on gold grains from Honduras gold placers.

2. Geological Background and Description of the Murcielago Gold Placer and Canan Lode Deposit

The geodynamic evolution of Honduras is the result of the complex interaction along a triple junction among the North American, Cocos, and Caribbean plates, which started in the Early Tertiary [22,23]. This interaction is responsible for the Central American subduction system, which consists of a northeast-directed slab subducting under two continental plates, i.e., the Caribbean and North American. The subduction is oblique to the plate boundary, and transpressional and transtensional tectonics are also active [24].

Honduras is placed on the NW minor crustal block of the Caribbean tectonic plate called Chortis Block, which has been referred to as the Precambrian-Paleozoic continental nucleus of the northern sectors of Central America [9,25]. According to the literature [23,25], the Chortis Block is not homogeneous and can be divided into different tectonic terranes. Its basement consists of metamorphic rocks with poorly constrained ages, ranging from Precambrian to Cenozoic, overlain by Meso-Cenozoic sedimentary and volcanic units. The sedimentary sequence consists of Middle Jurassic and Lower Cretaceous clastic sedimentary sequences, Lower Cretaceous carbonatic rocks, and Middle to Upper Cretaceous red beds and limestones intruded by Cretaceous and Tertiary granitic bodies. Cenozoic deposits largely consist of volcaniclastic rocks. The investigated area is located in the Lepaguare Valley (Olancho Department), about 100 km NE of Tegucigalpa (Figure 1). In this area, the basement is made up of low-grade metamorphic rocks represented by well-foliated

graphitic and sericitic schists and quartzites that can be referred to as the Cacaguapa Group. This Paleozoic basement is overlain by a relatively thick sequence of sedimentary rocks of roughly Jurassic to Cretaceous age, which includes two main units. The lower one consists of massive, dark-gray to black, strongly fractured limestones of the Lower Cretaceous age. This unit belongs to the Atima Formation, Yojoa Group [23], which crops out mainly in the mountains north of the Lepaguare Valley and to the south of the investigated area (Figure 1). The upper unit is instead represented by Upper Cretaceous redbed siliciclastic strata, which contain quartz-rich conglomerates, limestones, and minor evaporite rocks. The dominant lithologies are quartz pebble conglomerates, with poorly sorted, subangular to rounded quartz and quartzite pebbles in a fine red matrix. These strata belong to the Valle de Angeles Formation [25] that discontinuously crops out along the Guayape river. During the Upper Cretaceous–Lower Tertiary, these Mesozoic sedimentary units were intruded by a granodiorite pluton, which crops out a few tens of kilometers north and northwest of the Canan area. It corresponds to a medium-grained, equigranular, magnetite-bearing biotite-hornblende-granodiorite, varying locally to granite and quartz monzonite [9]. This intrusion is responsible for most of the metallogenic mineralizations within the Cacaguapa Shists (Figure 1). As described by [11–13,26], the Canan Lode gold deposit is associated with quartz-veined shear zones, and the mineralization occurs in the low-to medium-grade pre-Mesozoic metamorphic basement (graphitic and sericitic schists). Quartz veins were formed by hydrothermal fluids (associated with the emplacement of Cretaceous-Tertiary granodioritic intrusions) that altered the wall-rocks. Auriferous quartz vein formation is related to ductile shears and fault zones where hydrothermal fluids dominated by carbonate-chloride-bearing solutions and CO_2-CH_4-carbonic fluids circulated. The Murcielago gold placer is located along the Guayape river in the southern margin of the Lepaguare Valley (Figure 1). It represents a typical meandering channel deposit with a fining upward sequence. Coarser sediments are constituted by schists and granitoid rocks in a sandy–silty matrix comprising a wide variety of minerals.

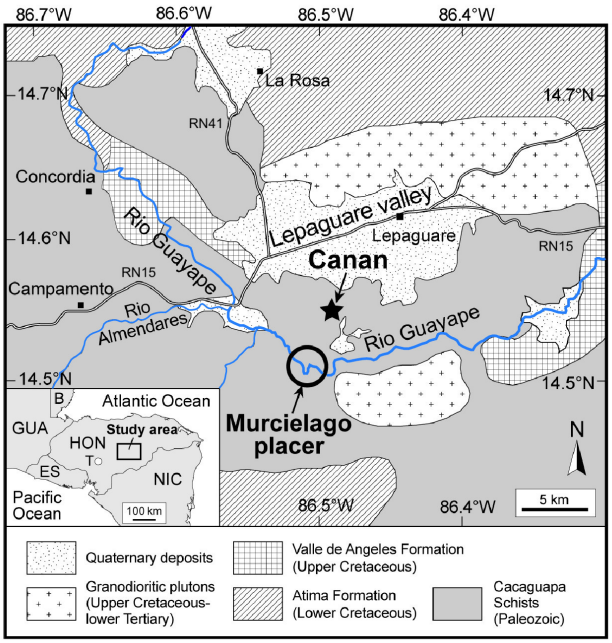

Figure 1. Geological sketch map of the investigated area of the Lepaguare Valley (Olancho Department) with the location of the Murcielago gold placer and the Canan lode deposit. Main geological units and fluvial system (in blue) are reported. RN = route number. Inset: GUA, Guatemala; B, Belize; HON, Honduras; ES, El Salvador; NIC, Nicaragua; T, Tegucigalpa city. Modified from [13].

3. Materials and Methods

3.1. Material Description

Gold grains from the Murcielago production plant and gold grains recovered after acid attack from the nearby Canan hydrothermal lode deposit were investigated. Concentrated and waste material from the Murcielago production plant were also analyzed to characterize the mineralogy of the sediment as a whole. Description and sample location are reported in Table 1.

Table 1. Sample location and details.

	Deposit Type	Location	Latitude	Longitude	Samples Number	Core Range At%
Canan	lode	from outcrop	14.55° N	86.5° W	6	$Au_{81}Ag_{19}$–$Au_{54}Ag_{44}$
Murcielago	placer	productive plant	14.5° N	86.5° W	34	$Au_{88}Ag_{12}$–$Au_{46}Ag_{54}$

This pilot production plant is based on a natural process of gold using mechanized separation and sorting after the excavation of the alluvial terrestrial material without any grinding step before the gravimetric concentration. The material is washed in pure water (without any chemicals) and separated by the combination of water and gravity only using sluices and spiral types of "centrifuge" machines.

3.2. Analytical Methods

Gold grains were investigated by optical microscopy on polished material embedded in epossidic resin under reflected light at 250× to 500× magnifications and using the electron microscope. Core and rim gold grains were quantitatively analyzed by electron microprobe with a Superprobe Jeol JXA 8200 at the Eugen F. Stumpfl Laboratory at Leoben University (Austria). The electron microprobe was operated in the wavelength dispersive X-ray spectrometry (WDS) mode at 25 kV accelerating voltage and 30 nA beam current. The beam diameter was about 1µm. The counting times for peak and background were 20 and 10 s, respectively, for Au and Ag, but they were increased up to 100 and 50 s during the analyses of trace elements, such as S, Fe, Co, Ni, Cu, Zn, As, Se, Sb, and Hg, to reduce the detection limits. The detection limits (wt.%) of the analyzed elements were automatically calculated by the microprobe software and they are: Au = 0.10, Ag = 0.045, As = 0.04, S = 0.03, Cu = 0.02, Ni = 0.02, Se = 0.03, Sb = 0.02, Fe = 0.01, Co = 0.01, Hg = 0.09, Zn = 0.02, and Te = 0.01. The analysis of S, Fe, Co, Ni, Cu, and Zn was carried out using the Kα lines; As, Se, Te, Ag, and Sb using Lα; and Au and Hg using Mα. The following analyzing crystals were used: TAP for As and Se; PETJ for S, Sb, and Hg; PETH for Au and Ag; and LIFH for Fe, Co, Ni, Cu, and Zn. Natural chalcopyrite, millerite, skutterudite, pyrite, stibnite, sphalerite, synthetic electrum, Pd_3HgTe_3, and $AgBiSe_2$ were used as reference material. Analyses are reported in Tables A1 and A2.

Semi-quantitative chemical analyses were carried out by scanning electron microscopy (SEM) on concentrated and waste material from the Murcielago production plant using an FE-SEM LEO 1525 Zeiss and a EDS detector Bruker Quantax 200 (equipped with an X-Flash 410 detector). To confirm the SEM-EDS identification of some minerals, a single-crystal X-ray diffraction (SC-XRD) was carried out by using an Xcalibur diffractometer (Rigaku) at the Department of Physics and Geology, University of Perugia. A short data collection routine of the CrysAlis 171.37.34 software (Rigaku) with parameters described in [27] was used to define the lattice parameters and identify the mineral.

The 2D morphometric analysis of the gold grains from the Murcielago placer was performed using optical microscopy photos. Small differences (<8%) arise from a 2D to 3D analysis if an image analysis software is used [20]. We carefully oriented all the gold grains with the flattest surface area on the glass plate before taking the microscopy photos. We defined

the grain contouring using the ImageJ 1.53K software (https://imagej.nih.gov/ij/index.html, e.g., downloaded on 22 March 2021 [28]) after processing the photos to obtain a black and white image. We approximated the shape of the grains to an ellipse and calculated the major and minor axes and the roundness (R) of each crystal.

4. Results

4.1. Placer Mineralogy

Placer mineralogy is characterized mainly by a silicate component and in minor amounts by phosphate, oxide, and rare sulfides. Quartz is the most abundant phase present in sediments. The silicate components in the sediments are garnet (stoichiometric andradite, grossular, and almandine), pale green hornblende amphibole, diopside-augite pyroxene, muscovite and biotite, epidote s.s., and tourmaline corresponding to dravite and schorl compositions, as confirmed by SC-XRD:

1. Shorl lattice parameters: a= 15.973(3) Åc = 7.158(6) Åsp. gr. R3m
2. Garnet lattice parameters: a = 12.064(2) Åsp. gr. Ia3d

The heavy minerals fraction is concentrated by the final process of gold concentration. Magnetite, haematite, ilmenite, and rutile are the most common opaque or semi-opaque heavy minerals. Ilmenite is present both as homogeneous crystals or with symplectitic textures. The composition is close to pure ilmenite, with only a minor substitution of pyrophanite ($MnTiO_3$) and geikielite ($MgTiO_3$) in the range $ilm_{88-97}pyr_{0-12}geik_{0-9}$. The exsolution of ilmenite and hematite and ilmenite-rutile intergrowths were also found. Zircon, monazite and xenotime, rutile, cassiterite, cinnabar, and rare pyrite and wolframite crystals are also present [29] (Tables A3–A5).

4.2. Gold Morphology and Chemistry

4.2.1. Gold from the Placer

We picked up gold grains by hand from the concentrated materials (grain size < 0.5 mm) of the Murcielago production plant. In this grain size class, the gold grains span between a few microns to 0.5 mm in size. The studied specimens were separated only using a shaking table at the production site and finally hand-picked, lowering as much as possible the artificial modification of the morphology of the gold grains. At first observation, the morphology of the gold grains is mainly a flattened type, with minor spherical types (Figure 2). The flattened grains type shows mainly a sub-circular shape, sometimes with folding and irregular morphology. We rarely found quasi-perfect spherical grains of the order of 100 µm in size.

Roundness was calculated as the ratio between minor and major ellipse axes: a round shape has an R value of 1, and for values of R < 1, we have an ellipse shape: the less the R value, the higher the eccentricity. With this approach, we obtained two end-members representing the flattened sub-circular type and a highly elliptical type. The approximation of the shape of the Murcielago gold grains is plotted in Figure 3. We can observe that most of the particles have an elliptical shape with an R value between 0.5 and 0.8 and that grains approximating a sub-circular morphotype are more frequent than highly elliptical grains. This type of approximation does not necessarily take into consideration the irregular shapes that we observed in the gold material; nevertheless, it roughly indicates the morphology of the grains.

The morphology of the polished gold grain sections revealed, together with the irregular, sub-circular, and elliptical shapes observed in the optical photos, the presence of porous structures and, rarely, Au-rich rims (Figure 4).

Moreover, a minor amount of gold grains associated with quartz (Figure 5) were recovered as well.

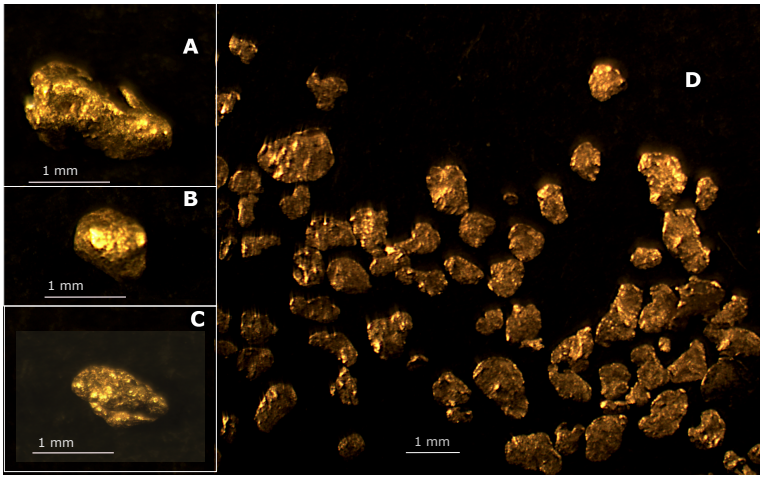

Figure 2. Gold with most common morphology of the Murcielago fluvial placer: (**A**–**C**) rounded-spherical type; (**D**) flattened-type grains.

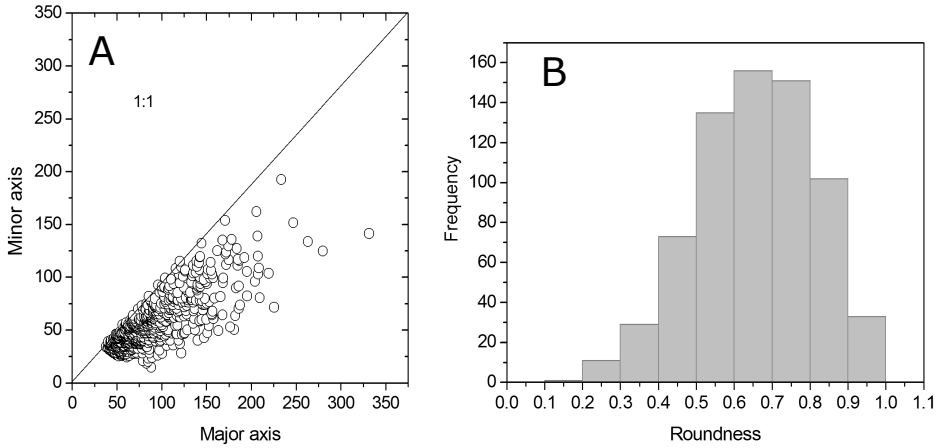

Figure 3. Analysis of the morphology of the Murcielago nuggets: (**A**) Major vs. minor axes (in pixel units) of the ellipse that approximates the nugget morphology (1:1 line representing circular shape is reported); (**B**) frequency distribution of the calculated roundness (see text for explanation).

Most of the Murcielago grains are actually chemically unzoned gold alloys with Ag between 12–54 atoms per cent (at%) with an asymmetric frequency distribution towards the highest Au values (Table A1, Figure 6). We rarely observed very enriched unzoned Au grains (Table A1). The few zoned grains are characterized by patchy zoning, different rim sizes, and porous structures, especially in the Au-rich rim zone (Figure 4, Table A1). The other elements component is, on average, very low, between 0 and 1.2 at%, with an exception of 3.14 at% (sample 1pH1, Table A1), which probably reflects the presence of a tiny, not detected inclusion of Cu, since this element is generally below the detection limit except for this point.

Inclusions in gold particles from surficial environments are rare and vary in frequency, decreasing with the degree of fluvial transport and particle flattening. Thus, the probability to find inclusions in polished material is estimated to be around 10% [30]. In the placer material, we found only two grains with tiny inclusions visible on the polished surface (Figure 6).

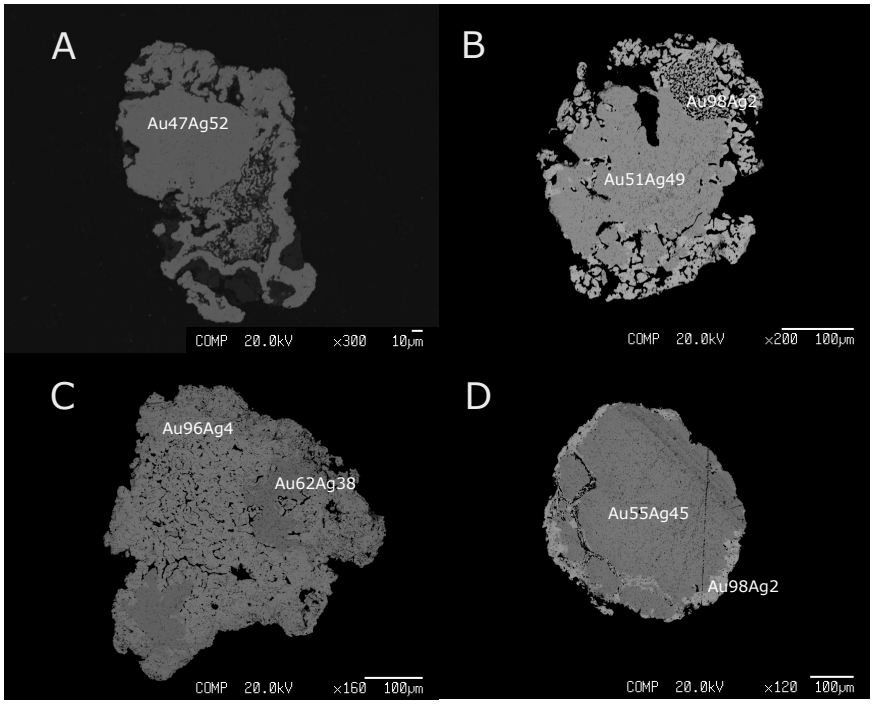

Figure 4. SEM back scattering secondary electron images of the Murcielago gold grains: brighter and less bright areas emphasize higher and lower Au concentrations, respectively. Alloy composition in at% is reported. (**A**) Homogeneous 2pH1 sample; (**B**) patchy zoned 2pA sample; (**C**) zoned 2pI sample with irregular rim; (**D**) zoned 2pE sample with very thin rim.

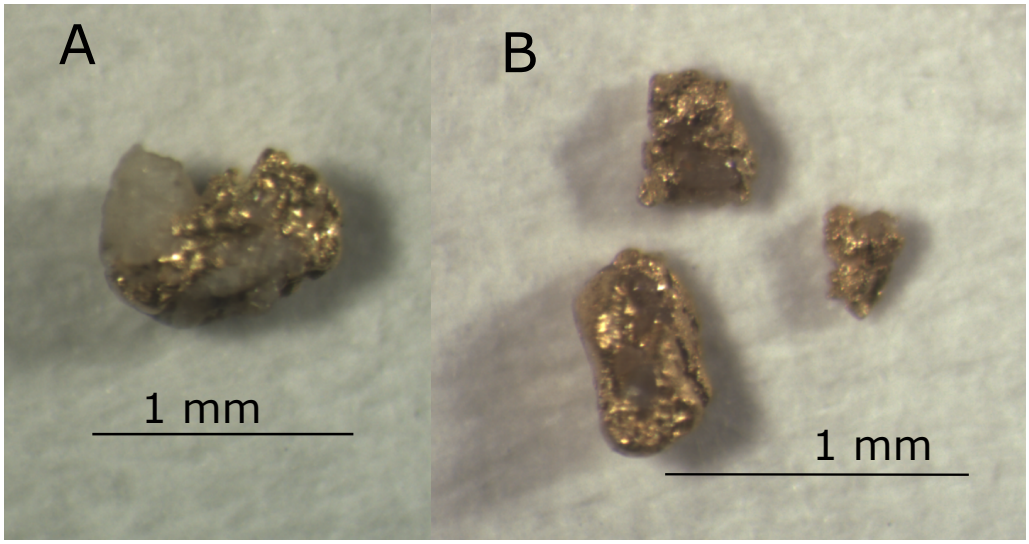

Figure 5. (**A**,**B**) Gold grains associated with quartz from the Murcielago placer.

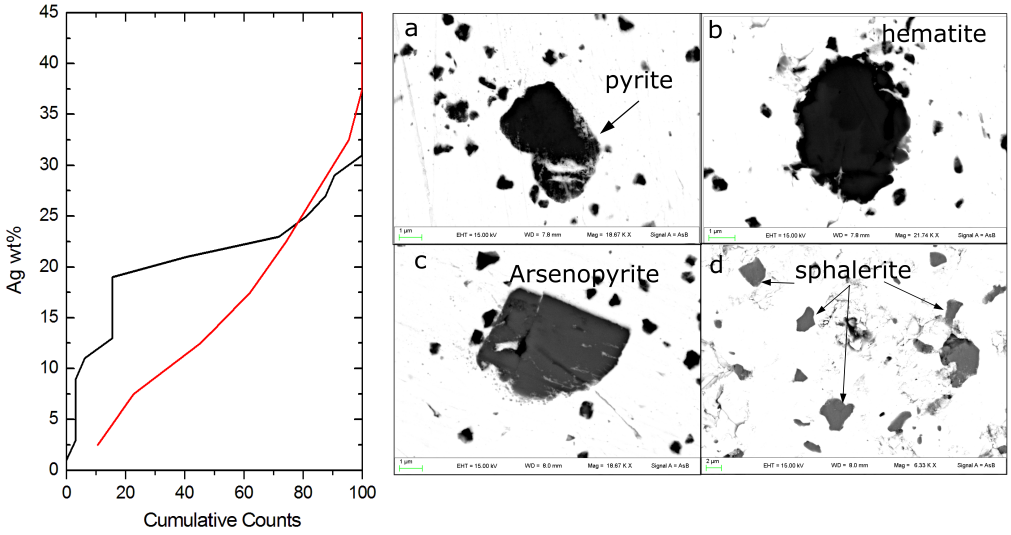

Figure 6. Cumulative counts vs Ag content (wt%) of the Murcielago gold (red line) and the Canan lode gold (black line). (**a**–**d**) SEM images of ore-mineral inclusions in Murcielago gold grains. (**a**) pyrite; (**b**) hematite; (**c**) arsenopyrite; (**d**) sphalerite.

SEM-EDS measurements are compatible (despite being altered) with pyrite, arsenopyrite, sphalerite, and hematite (Figure 6). Trails of acanthite crystals (Ag_2S) can be observed in the map of Figure 7. Grain1 of composition $Au_{55}Ag_{45}$ hosts inclusions of arsenopyrite, whereas grain2 of composition $Au_{64}Ag_{36}$ hosts an association of pyrite, acanthite, sphalerite, and hematite as inclusions (Table A6).

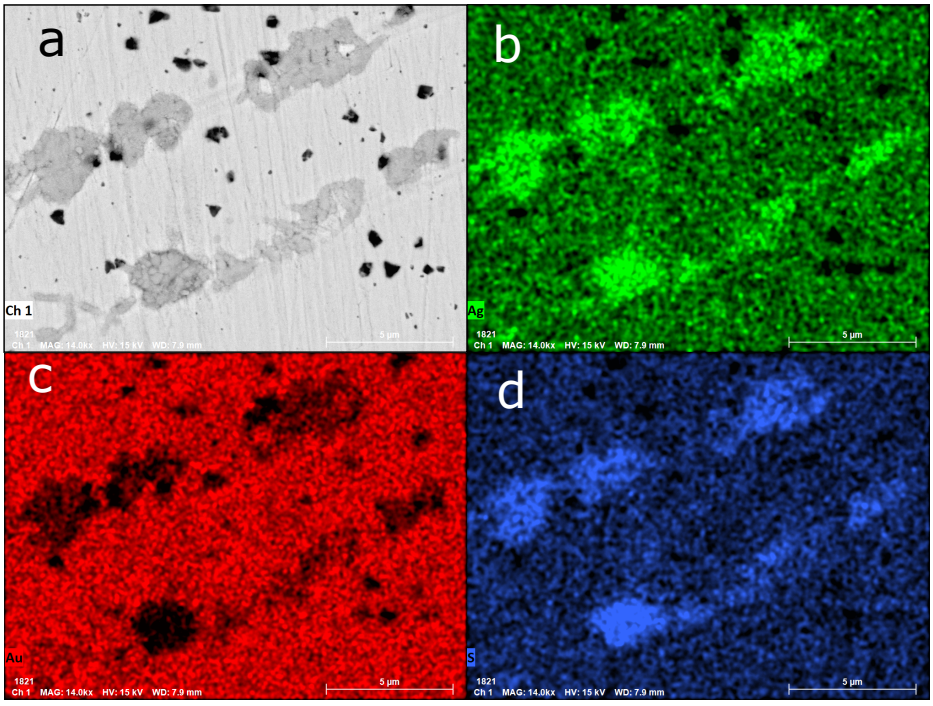

Figure 7. SEM-EDS maps of acanthite inclusion in gold grain2. (**a**) BSE image; (**b**) silver; (**c**) gold; (**d**) sulfur. Acanthite chemical composition is reported in Table A6.

4.2.2. Gold from the Canan Lode

The Canan gold grains have a diameter size between 2 µm and 1 mm and show ovoid, spherical, or elongated morphology [13]. Gold grains from Canan are porous crystals (Figure 8), and, unfortunately, this feature influenced the specimen preparation for the

quantitative electron microprobe analysis and the quality of the data. Gold grains from the Canan lode deposit are unzoned gold alloys with a composition varying from $Au_{53}Ag_{46}$ to $Au_{79}Ag_{20}$ (average $Au_{72}Ag_{37}$) (Table A2). Other element content is generally very low to absent: Cu is below the detection limit, while Fe is detected in all the analyzed grains. The other trace elements (S, Zn, Ni,Te) are not always present (Table A2). No inclusions can be observed in the Canan material because of the low amount of material available.

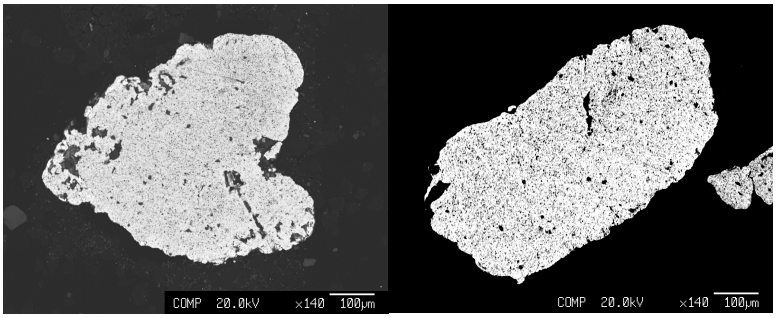

Figure 8. SEM back scattering secondary electron images of gold grains from Canan lode deposit.

5. Discussion

The Murcielago gold deposit is a placer located along the Guayape river. The meandering channel deposit is the result of the erosion of the Guayape river in the hydrographic basin, which is characterized by a sequence of schists, redbeds siliciclastic, and granitoid rocks. Evidence of metallogenic mineralization is reported at the schists level. The placer mineralogy reflects the complex lithology of the area where the Guayape river is located (Figure 9). The presence of key minerals, such as epidote, tourmaline, and garnet end-members (almandine, grossular, and andradite), as well as biotite and phlogopite, monazite, xenotime, and zircon, suggests a provenance from metamorphic and granodioritic lithologies of the area and the relative mineralized rocks (i.e., Cu–Au skarn) from the nearby ore district [5,9,15]. In particular, accessory minerals of the granodioritic rocks (i.e., monazite, xenotime, and zircon) and the presence in the heavy fractions of metal oxide and sulfide, such as cassiterite, wolframite, and altered pyrite, suggest that the sediments of the Guayape river are mainly linked to the erosion of the mineralized units of the Cacaguapa Schists.

Although several mineralized units are reported in the area, the lode gold source of the Murcielago placer is still unknown. Cu–Au skarn and hydrothermal lode deposits are the only known gold mineralization in the area [9,12,13], and thus, they could be the best candidate source for the Murcielago gold placer.

The gold grains recovered from the Murcielago placer production plant are mainly flattened grains, and from the morphometric analysis, they resulted in moderately to high elliptical shape (Figure 2). As observed by Masson et al. [20], gold grains sampled at different distances from the lode deposit in the Rivière du Moulin (Québec, Canada) have no significant change in flatness with the distance of transport (up to 10 km) or roundness along the river. By contrast, a slight decrease in ellipticity, from high to moderately elliptic particles, and an increase in roundness, from moderately to highly rounded, with distance are reported. Nevertheless, they suggested that the observed grain morphology can be affected not only by the distance of transport but also by multiple gold sources. Since our samples come from a single production site, and we observe a significant spread in the shape descriptors (including rough gold grains plus quartz), a possible hypothesis (in analogy with [20]) is that some gold particles may have traveled longer than the others, implying a variable distance from one or multiple sources. Nevertheless, to confirm this hypothesis, further analysis considering the alloy composition of the sub-population will be necessary.

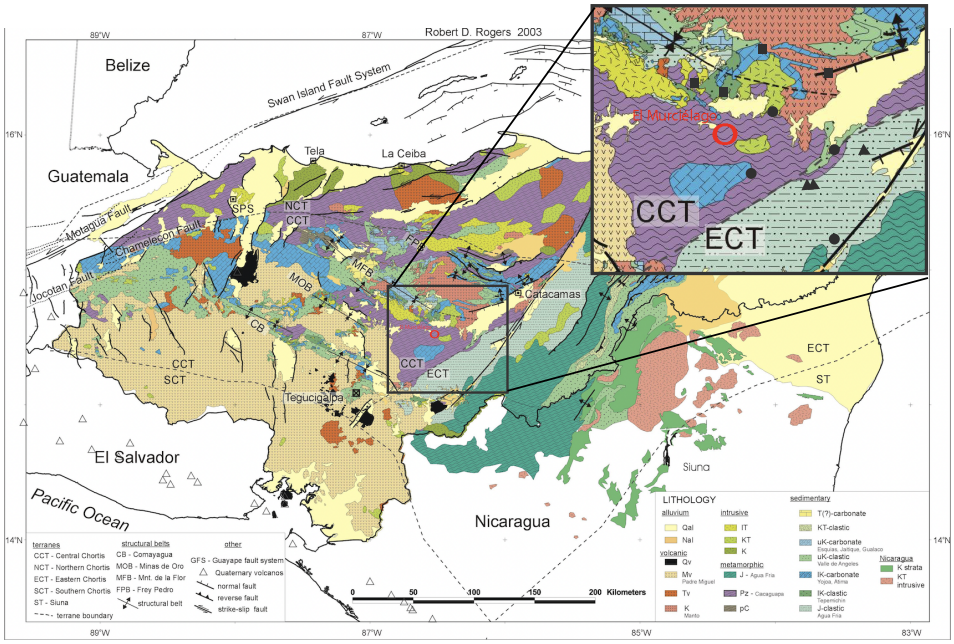

Figure 9. Geological map of Honduras modified from [25]. In the inset the gold deposits of the studied area are shown [14]: triangle = orogenic deposits; square = skarn deposits; circle = epithermal deposits.

Recently, Chapman et al. [31] reported a comprehensive study on alluvial gold from a huge placer gold database from locations worldwide in determining the contributions of detrital and authigenic gold to fluvial placers. Murcielago gold alloy varies continuously in the $Au_{55}Ag_{45}$–$Au_{88}Ag_{12}$ range, as measured at the core of the grains. The compositional range can be considered primary and ascribed both to a variation in the precipitation conditions present in the source (temperature or pH variation of Au concentration, aH_2S and aCl^-(aq); increase in Ag in the alloy) and/or to multiple sources.

The lode deposits present in the area of Canan are the only hypogene deposits of which we had samples. No chemical analyses of gold composition are reported in the literature as far as we know. Thus, inferring a possible source is extremely difficult, but we can make some comparison with the nearby Canan deposit. Although the cumulative curves for Canan and Murcielago slightly differ (Figure 6), the composition of Canan gold grains ($Au_{53}Ag_{46}$–$Au_{79}Ag_{20}$) overlaps that of the Murcielago placer. The limited amount of Canan samples analyzed prevents better describing the possible difference between the two populations. Moreover, as reported by Chapman et al. [31], the gold alloy major composition alone cannot discriminate between different sources. Few grains from the Murcielago placer have an Au-rich rim of a few microns thick (Figure 4). The presence of Au-rich rims in placer gold grains is usually secondary and related to the micron-scale overgrowth of pure Au or to Ag depletion processes that can occur during the history of the gold from the source to the placer deposit [30,32]. The thickness of the Au-rich rim depends on the pristine condition before the particle enters the fluvial system and/or the residence time in the system itself. Generally, the Ag-depleted inner rim has a thickness of around 20 µm and a geometry broadly mirroring the particle edge.

In our case, rim composition is around 1–2 at% Ag and, together with the morphology of the grains, may be compatible with Ag removal processes possibly during the residence in the placer. Some additional information can be obtained from the analysis of the inclusions present in the polished section and the finding of gold grains associated with quartz found in the concentrated material. The observed mineral inclusions did not present a void between the host gold and the ore mineral, thus suggesting a primary origin. The association is arsenopyrite, pyrite, acanthite, sphalerite, and hematite. In particular, pyrite and sphalerite are very common in several styles of mineralization (e.g., orogenic, skarn, and epithermal gold) and could not be discriminant on one or more sources [30,31,33].

Moreover, the inclusions are found in gold grains of a similar composition ($Au_{55}Ag_{45}$ and $Au_{64}Ag_{36}$) but with the few available data, we cannot unambiguously define them as a single or multiple gold types. Nevertheless, pyrite, arsenopyrite, sphalerite, goethite, and hematite are among the ore minerals present in the Canan gold deposits, and the Murcielago chemistry of gold grains with inclusions is also compatible with the Canan gold composition. We did not observe mineral inclusions in the Canan gold grains, probably because of the scarcity of available materials. Moreover, the observed gold grains with associated quartz are in the 1 mm to 0.4 mm range and look primary, therefore suggesting a proximal source where gold is associated with quartz.

6. Conclusions

Data from the literature on gold from ore deposits of Honduras are extremely scarce, and gold compositions are lacking, with the exception of those reported by [13] for the Canan lode deposits. In this study, we report the first data on the chemical characterization of the Murcielago gold placer and a comparison with gold from the Canan lode deposit in the Olancho Department. The morphology range of the placer gold grains, their chemical composition, and the substantial lack of extensive Ag depletion suggest that the gold may have been transported from variable distances and possibly from multiple sources.

The presence of gold associated with quartz in the placer materials and the ore mineral inclusions observed in the gold grains give new constraints to the possible source(s) that should be searched for the gold deposits present in the hydrographic drainage of the Guayape river (Figures 1–9), although a poor knowledge of the gold deposits in the district makes it more difficult to infer which is/are the source(s) of the Murcielago gold placer. In this way, we tentatively compared the composition of gold from the Canan lode and the placer deposits, which resulted consistently.

Although the hydrographic drainage of the Canan gold deposits could not be directly related to the Murcielago placer, it is conceivable that, further west-southwest, some tributaries of the Guayape river, just a few kilometers upstream from the Murcielago alluvial sediments, cut, within the widespread Cacaguapa schists, some hydrothermal gold mineralization genetically similar to that of Canan. Moreover, the presence of andradite garnet, pyrite, and magnetite in the concentrated material of the Murcielago placer seems to suggest that Cu–Au skarn deposits of the Cagaguapa schists could be an additional candidate source for the investigated placer.

Author Contributions: Conceptualization, S.N. and M.M.; methodology, S.N. and F.Z.; software, S.N.; formal analysis, S.N., S.A., A.D.M. and F.Z.; investigation, S.N., S.A., A.D.M. and F.Z.; writing—original draft preparation, S.N., A.R. and M.M.; writing—review and editing, S.N., A.R., M.M., A.M. and F.Z.; project administration, S.N. All authors have read and agreed to the published version of the manuscript.

Funding: This research received no external funding.

Institutional Review Board Statement: Not applicable.

Informed Consent Statement: Not applicable.

Data Availability Statement: Original data are reported in Appendix A and can be obtained by the corresponding author upon request.

Acknowledgments: Giuseppe Colaiacovo and Goldlake Group Company are greatly acknowledged for providing the samples. Luca Bartolucci is thanked for the SEM analysis at the Department of Physics and Geology of Perugia University. The University Centrum for Applied Geosciences (UCAG) of University of Leoben, Austria, is thanked for the access to the Eugen F. Stumpfl electron microprobe laboratory. The editor and reviewers are greatly acknowledged for discussion and suggestions.

Conflicts of Interest: The authors declare no conflict of interest.

Appendix A. The Ethical Gold: A Sustainable Mining Example of the Murcielago Placer

The Murcielago pilot mining project was developed by the Goldlake Group in 2004 (through the subsidiary Eurocantera), aiming to create a sustainable gold mining model starting from their experience in the concrete industry. The mining project was characterized by environmental, social, and governance programs and severe control of the whole supply chain, following the best practice requested by the Responsible Jewellery Council (RJC). The Goldlake Group obtained the RJC certificate for the gold coming from the Murcielago area then called "Ethical Gold". Later on, in 2018, this project resulted in the "Makal" enterprise, ethical gold nuggets and fine gold jewelry by Daniela Colaiacovo (founder and CEO). The main points of the mining project regarded the environmental aspects targeting a positive balance between before and after exploitation with a continuous reclamation program by the creation of fruit-bearing plantations; social aspects with the banning of labor by minors and pregnant women, associated with a strong local collaboration and investments in education and health; and economic and financial aspects with a specific part of the project. In particular, the maintenance of a controlled balance between the recovery and loss of gold from the production plant avoided the use of cyanide and the high final costs of environmental remediation, such as dams and settling ponds and cyanide recovery. The entire mining area was explored by progressive exploration and exploitation of horizontal layers with large trenches (bulk samples of 500 tons) located in a mesh network determined by the geological survey after assaying each level. Specimens excavated on the trenches were sent to the pilot laboratory to be concentrated, without any grinding step, by using uniquely gravimetric separation methods so that the gold grade for each layer was determined. The obtained data allowed selective exploitation of the mine to be carried out. The alluvial terrestrial material was excavated, using a mechanized separation and sorting step before the gravimetric concentration. The material was washed in pure water (without any chemicals, cyanide, or harmful chemicals) and separated by the combination of water and gravity by only using different types of "centrifuge" machines with a tabular and spiral morphology.

Table A1. Chemical composition of the gold grains from the Murcielago placer. Major oxides and trace elements are reported in wt% and recalculated in at%. Detection limits are reported in the text.

Wt%	**2pAcore1**	**2pArim2**	**2pArim3**	**2pB1**	**2pB2**	**2pC1**	**2pC2**	**2pD1**	**2pD2**	**2pEcore1**	**2pErim2**	**2pF2**
Au	65.54	100.78	101.33	75.71	74.26	71.92	70.77	86.98	87.71	69.79	99.61	84.86
Ag	33.95	1.27	1.00	25.85	26.64	30.51	28.87	13.42	13.22	31.05	1.26	16.64
Sb	–	0.03	–	–	–	–	–	–	–	–	–	–
Fe	–	0.02	0.10	–	–	–	–	–	–	–	0.02	–
Zn	–	0.03	–	–	–	–	–	–	–	–	–	–
Te	0.05	0.02	0.02	0.05	0.05	0.04	0.07	0.04	–	0.06	–	0.04
Total	99.54	102.16	102.44	101.61	100.95	102.47	99.71	100.95	100.93	100.90	100.88	101.53
At%												
Au	51.39	97.53	97.88	61.59	60.42	56.36	57.29	77.65	78.44	55.18	97.68	73.63
Ag	48.54	2.24	1.76	38.35	39.52	43.60	42.62	21.85	21.56	44.76	2.24	26.32
Sb	–	0.05	–	–	–	–	–	–	–	–	–	–
Fe	–	0.07	0.33	–	–	–	–	–	–	–	0.07	–
Zn	–	0.08	–	–	–	–	–	–	–	–	–	–
Te	0.07	0.03	0.03	0.06	0.06	0.05	0.09	0.06	–	0.07	–	0.05
Total	100.00	100.00	100.00	100.00	100.00	100.00	100.00	100.00	100.00	100.00	100.00	100.00
Wt%	**2pG1**	**2pG2**	**2pH1**	**2pIcore1**	**2pIcore2**	**2pIrim3**	**2pL1**	**2pMcore1**	**2pMrim3**	**2pN1**	**2pO1**	**2pO2**
Au	66.89	65.34	62.95	75.76	76.50	98.94	83.27	79.91	100.83	92.05	84.64	83.39
Ag	34.60	34.51	37.93	25.17	25.17	2.20	16.11	20.24	0.72	9.66	17.26	16.68
Sb	–	–	0.16	–	–	–	–	–	–	0.04	–	–
Fe	–	–	–	–	–	–	–	–	–	–	–	0.02
Te	0.10	0.08	0.05	0.05	0.07	–	0.06	0.05	–	–	0.03	0.04
Total	101.58	99.93	101.09	101.01	101.74	101.14	99.43	100.20	101.56	101.76	101.93	100.13
At%												
Au	51.40	50.89	47.53	62.19	62.45	96.10	73.86	68.36	98.71	83.88	72.87	73.19
Ag	48.49	49.01	52.22	37.67	37.46	3.90	26.06	31.57	1.29	16.06	27.09	26.70
Sb	–	–	0.192	–	–	–	–	–	–	0.065	–	–
Fe	–	–	–	–	0.037	–	–	–	–	–	–	0.058
Zn	–	–	–	0.08	–	–	–	–	–	–	–	–
Te	0.11	0.09	0.06	0.06	0.09	–	0.08	0.07	–	–	0.04	0.05
Total	100.00	100.00	100.00	100.00	100.00	100.00	100.00	100.00	100.00	100.00	100.00	100.00

Table A1. *Cont.*

Wt%	**2pO3**	**2pP1**	**2pP2**	**2pP4**	**2pQ1**	**2pQ2**	**2pR1**	**2pR2**	**2pS2**	**2pT2**	**2pT3**	**2pU1**
Au	79.22	77.34	84.34	82.06	86.45	86.97	73.29	74.16	94.25	79.84	78.16	84.37
Ag	20.43	23.04	16.99	18.14	12.44	12.72	25.45	26.68	7.94	21.78	21.28	16.69
Hg	–	–	–	–	–	1.08	–	–	–	0.43	0.13	–
Zn	–	0.03	–	–	–	–	–	–	–	–	–	0.04
Te	0.05	0.03	0.05	0.02	0.02	0.06	–	0.05	–	0.05	0.04	0.03
Total	99.69	100.45	101.38	100.23	99.83	100.84	98.75	100.89	102.18	102.10	99.63	101.12
At%												
Au	67.99	64.72	73.08	71.25	78.54	78.13	61.23	60.35	86.69	66.50	66.68	73.40
Ag	31.96	35.16	26.85	28.72	20.61	20.84	38.77	39.58	13.31	33.08	33.10	26.47
Hg	–	–	–	–	0.82	0.95	–	–	–	0.35	0.11	–
Zn	–	0.08	–	–	–	–	–	–	–	–	–	0.10
Te	0.06	0.04	0.07	0.03	0.03	0.08	–	0.07	–	0.07	0.05	0.04
Total	100.00	100.00	100.00	100.00	100.00	100.00	100.00	100.00	100.00	100.00	100.00	100.00
Wt%	**2pU2**	**2pV1**	**1pA2**	**1pA3**	**1pB1**	**1pB3**	**1pC1**	**1pC2**	**1pC3**	**1pD2**	**1pD3**	**1pD4**
Au	81.89	97.74	78.38	77.20	60.18	61.39	90.17	90.28	92.24	94.50	94.49	90.52
Ag	16.28	2.63	19.43	21.19	39.02	38.13	9.66	10.03	9.80	8.00	8.00	8.09
Fe	0.02	–	–	–	–	0.04	–	–	–	–	–	0.02
Zn	–	–	–	–	–	–	–	–	–	–	0.03	–
Te	0.03	–	0.06	0.02	0.07	0.06	0.04	0.02	–	0.03	–	0.04
Total	98.22	100.38	97.86	98.41	99.26	99.62	99.86	100.34	102.03	102.53	102.53	98.67
At%												
Au	73.29	95.32	68.82	66.63	45.78	46.81	83.62	83.12	83.78	86.59	86.54	85.89
Ag	26.58	4.68	31.10	33.34	54.14	53.01	16.33	16.85	16.22	13.37	13.36	13.99
Fe	0.05	–	–	–	–	0.10	–	–	–	–	–	0.06
Zn	–	–	–	–	–	–	–	–	–	–	0.09	–
Te	0.05	–	0.08	0.03	0.08	0.07	0.05	0.03	–	0.04	–	0.06
Total	100.00	100.00	100.00	100.00	100.00	100.00	100.00	100.00	100.00	100.00	100.00	100.00

Table A1. *Cont.*

Wt%	**1pD5**	**1pE1**	**1pF1**	**1pF2**	**1ptF3**	**1pF4**	**1pG1**	**1pH1**	**1pI1**	**1pI2**	**1pM2**	**1pM3**
Au	93.47	88.74	88.80	88.64	88.19	89.00	76.31	96.20	81.53	80.75	88.74	89.58
Ag	7.01	12.36	12.46	12.14	12.23	12.68	22.18	1.47	18.17	17.93	10.80	11.36
S	–	–	–	–	–	–	–	0.06	–	–	–	–
Cu	–	–	–	–	–	–	–	1.04	–	–	–	–
Sb	–	–	–	–	–	–	–	–	–	–	–	0.04
Fe	–	–	0.03	–	–	–	–	–	–	–	–	0.02
Hg	–	–	–	–	–	–	–	–	0.40	1.02	–	–
Te	–	0.02	0.02	–	0.02	–	0.05	–	0.05	–	–	0.03
Total	100.48	101.12	101.30	100.77	100.44	101.72	98.54	98.77	100.15	99.70	99.54	101.03
At%												
Au	87.97	79.73	79.54	80.02	79.79	79.30	65.31	93.91	70.82	71.56	81.84	81.09
Ag	12.03	20.25	20.36	19.98	20.18	20.61	34.62	2.61	28.77	28.56	18.16	18.75
S	–	–	–	–	–	–	–	0.34	–	–	–	–
Cu	–	–	–	–	–	–	–	3.14	–	–	–	–
Sb	–	–	–	–	–	–	–	–	–	–	–	0.06
Fe	–	–	0.8	–	–	–	–	–	–	–	–	0.06
Hg	–	–	–	–	–	–	–	–	0.34	0.88	–	–
Te	–	0.02	0.02	–	0.03	–	0.06	–	0.07	–	–	0.04
Total	100.00	100.00	100.00	100.00	100.00	100.00	100.00	100.00	100.00	100.00	100.00	100.00

Wt%	**1pN1**	**1pN2**	**1pO2**	**1pP1**	**1pP2**	**1ptQ1**
Au	64.34	67.61	83.51	88.04	86.32	71.09
Ag	34.39	30.76	13.64	12.28	11.05	21.57
Fe	–	–	–	–	–	0.02
Hg	0.57	–	–	0.57	0.13	–
Zn	–	–	0.03	–	–	–
Te	0.04	0.06	0.06	0.04	0.02	0.04
Total	99.33	98.43	97.24	100.92	97.52	92.72
At%						
Au	50.40	54.62	76.93	79.28	80.95	64.31
Ag	49.12	45.31	22.91	20.17	18.90	35.58
Fe	–	–	–	–	–	0.06
Hg	0.44	–	–	0.50	0.12	–
Zn	–	–	0.08	–	–	–
Te	0.05	0.07	0.09	0.05	0.02	0.05
Total	100.00	100.00	100.00	100.00	100.00	100.00

Table A2. Chemical composition of the gold grains from Canan gold lode deposit. Major oxides and trace elements are reported in wt% and recalculated in at%. Detection limits are reported in the text.

wt%	LodeG1-4	LodeG1-6	LodeG1-8	LodeG1-9	LodeG2-1	LodeG2-3	LodeG3-4	LodeG3-5	LodeG3-6	LodeG3-7
Ag	12.84	10.95	12.74	12.02	30.62	30.18	23.26	28.26	27.66	23.90
Au	83.76	86.99	84.83	85.83	66.49	67.74	74.30	70.61	73.27	74.57
S	-	0.09	0.04	0.04	-	0.42	0.07	0.06	0.04	0.06
Fe	0.05	0.03	0.07	0.04	0.07	0.07	0.10	0.05	0.03	0.06
Zn	-	-	0.03	-	0.04	0.03	-	-	-	0.03
Te	0.04	-	0.05	-	0.06	0.04	0.03	0.04	0.07	0.06
Total	96.70	98.06	97.74	97.93	97.29	98.47	97.77	99.03	101.07	98.69
at%										
Ag	21.80	18.58	21.37	20.27	45.48	43.76	36.07	41.98	40.61	36.65
Au	77.97	80.83	78.06	79.36	54.16	53.87	63.20	57.52	59.00	62.69
S	-	0.50	0.20	0.24	-	2.06	0.39	0.29	0.21	0.31
Fe	0.17	0.11	0.23	0.13	0.19	0.19	0.31	0.15	0.09	0.18
Zn	-	-	0.08	-	0.09	0.08	0	0	0	0.09
Te	0.06	-	0.06	-	0.07	0.04	0.04	0.05	0.08	0.08
Total	100	100	100	100	100	100	100	100	100	100
wt%	**LodeG4-2**	**LodeG4-3**	**LodeG4-5**	**LodeG4-7**	**LodeG4-8**	**LodeG4-10**	**LodeG5-3**	**LodeG5-5**	**LodeG5-6**	**LodeG5-8**
Ag	20.81	21.02	22.10	23.44	21.35	22.48	20.72	20.79	21.38	22.08
Au	77.19	75.20	78.51	77.15	75.38	75.53	76.19	74.86	75.82	76.76
S	-	-	0.05	0.04	-	-	0.14	0.08	-	0.10
Fe	0.04	0.03	0.03	0.48	0.05	0.05	0.06	0.14	0.05	0.07
Zn	-	0.03	0.05	-	0.03	-	-	-	0.03	0.03
Te	0.03	0.03	0.03	0.05	-	0.02	0.03	0.02	0.02	0.03
Total	98.08	96.31	100.78	101.16	96.82	98.07	97.15	95.92	97.30	99.07
at%										
Ag	32.90	33.69	33.75	35.06	33.98	35.15	32.83	33.30	33.87	34.12
Au	66.93	66.08	65.73	63.28	65.77	64.67	66.20	65.76	65.88	65.03
S	-	-	0.24	0.20	-	-	0.74	0.41	-	0.54
Fe	0.13	0.10	0.10	1.40	0.17	0.15	0.19	0.42	0.15	0.20
Zn	0.01	0.09	0.13	-	0.08	-	-	-	0.07	0.07
Te	0.04	0.04	0.04	0.06	-	0.02	0.05	0.03	0.03	0.04
Total	100	100	100	100	100	100	100	100	100	100

Table A2. *Cont.*

wt%	LodeG6-1	LodeG6-3	LodeG6-4	LodeG6-5	LodeG6-9	LodeG6-10
Ag	24.20	24.92	23.80	26.62	23.94	25.19
Au	76.49	75.38	73.79	73.49	73.05	73.80
S	0.06	-	0.12	0.06	0.13	0.04
Fe	0.06	0.04	0.04	0.05	0.04	0.09
Zn	0.05	-	0.03	0.04	-	0.04
Te	0.04	0.02	0.04	0.05	-	0.08
Total	100.90	100.36	97.82	100.31	97.16	99.23
at%						
Ag	36.35	37.56	36.72	39.54	37.11	38.11
Au	63.01	62.30	62.42	59.86	62.09	61.23
S	0.30	-	0.64	0.31	0.68	0.20
Fe	0.16	0.12	0.11	0.14	0.11	0.26
Zn	0.11	-	0.06	0.09	-	0.10
Te	0.06	0.03	0.05	0.06	-	0.10
Total	100	100	100	100	100	100

Table A3. Selected EDX chemical compositions of minerals from the Murcielago placer. Major oxides are reported in wt%.

	Tourmaline			Amphibole	Muscovite	Biotite	Andradite	Almandine	Epidote
	Cx4	Cx5	Cx7						
Na_2O	2.42	2.34	1.29	1.16	0.09	0.37	–	–	–
MgO	3.13	10.54	4.26	17.45	0.96	2.23	–	–	–
Al_2O_3	32.94	31.55	22.98	8.32	35.48	30.1	3.47	25.26	22.74
SiO_2	35.33	37.36	37.09	51.94	48.11	47.18	34.34	33.38	38.8
CaO	–	1.1	0.5	12.33	–	–	38.02	–	23.05
FeO	–	–	–	8.7	1.87	7.18	–	–	–
Fe_2O_3	13.18	4.12	20.87	–	–	–	24.17	41.37	15.42
TiO_2	–	–	–	0.11	–	–	–		–
K_2O	–	–	–	–	9.28	8.94	–	–	–
Total	87	87	87	100	95.78	96	100	100	100

Table A4. Selected EMPA analysis representative of ilmenite and magnetite composition from the Murcielago placer. Major oxides are reported in wt%.

	Cx 1	Cx2	Cx3	Cx4	Cx5	Cx6	Cx7	Cx8
TiO_2	45.81	44.02	67.58	62.16	67.58	67.58	56.4	53.56
FeO	52.7	54.72	26.08	32.47	26.08	26.08	38.77	44.73
MnO	1.49	1.25	6.34	5.37	6.34	6.34	4.38	1.7
Totale	100	99.99	100	100	100	100	99.55	99.99

Table A5. Selected EDX analysis representative of monazite and xenotime compositions from the Murcielago placer. Major oxides are reported in wt%.

	Monazite	Xenotime
P_2O_5	36.02	52.29
ThO_2	3.33	–
La_2O_3	8.22	–
Ce_2O_3	36.84	–
Nd_2O_3	15.59	–
Y_2O_3	–	47.71
Total	100	100

Table A6. EDX analysis (in At%) representative of ore mineral inclusions found in gold grains from the Murcielago placer.

	Arsenopyrite Gold1c	Arsenopyrite Gold1b	Pyrite Gold 2d	Pyrite Gold2c
Fe	36.87	35.21	35.92	35.62
As	36.31	41.65	-	-
S	26.82	23.14	64.08	64.18
Ag	-	-	-	0.20
Total	100	100	100	100
	Acanthite Gold2e			
Ag	61.35			
S	38.65			
Total	100			

Table A6. *Cont.*

	Sphalerite Gold 2g	**Sphalerite Gold2b**
Zn	62.68	60.95
Hg	3.28	3.54
S	34.04	35.51
Total	100	100
	Hematite Gold2a	**Hematite Gold2b**
Fe	59.79	63.00
Mn	0.33	0.45
O	39.88	36.56
Total	100	100

References

1. Kesler, S. Metallogenesis of the Caribbean region. *J. Geol. Soc.* **1978**, *135*, 429–441. [CrossRef]
2. Sundblad, K.; Cumming, G.; Krstic, D. Lead isotope evidence for the formation of epithermal gold quartz veins in the Chortis Block, Nicaragua. *Econ. Geol.* **1991**, *86*, 944–959. [CrossRef]
3. Nelson, C.E.; LÓpez-Kramer, J.; Lewis, J.F.; Proenza, J. The metallogenic evolution of the Greater Antilles. *Geol. Acta Int. Earth Sci. J.* **2011**, *9*, 229–264.
4. Kesler S.E.; Levy E.M.C. *Metallogenic Evolution of the Caribbean Region*; Geological Society of America, Inc.: Boulder, CO, USA , 1990; Volume H, pp. 459–482.
5. U.S. Geological Survey. *Mineral Resources Data System*; U.S. Geological Survey: Reston, VA, USA, 2023. Available online: https://mrdata.usgs.gov/mrds/ (accessed on 11 March 2023).
6. Roberts, R.J.; Irving, E.M. *Mineral Deposits of Central America*; US Government Printing Office: Washington, DC, USA, 1957; Volume 1034.
7. Carpenter, R.H. Geology and ore deposits of the Rosario mining district and the San Juancito Mountains, Honduras, Central America. *Geol. Soc. Am. Bull.* **1954**, *65*, 23–38. [CrossRef]
8. Svandholm, J. Gold in Honduras. In *Where to Look and Find It*; World Mining: Butte, MT, USA, 1975; pp. 30–31.
9. Drobe, J.; Cann, R.M. Cu-Au Skarn Mineralization, Minas de Oro District, Honduras, Central America. *Explor. Min. Geol.* **2000**, *9*, 51–63. [CrossRef]
10. Williams-Jones, A.; Samson, I.; Ault, K.; Gagnon, J.; Fryer, B. The genesis of distal zinc skarns: Evidence from the Mochito deposit, Honduras. *Econ. Geol.* **2010**, *105*, 1411–1440. [CrossRef]
11. Menichetti, M.; Mattioli, M.; Renzulli, A.; Salvioli-Mariani, E.; Martens, U. Contesto strutturale, mineralogia e geochimica di giacimenti auriferi in Honduras Centrale. *Rend Soc Geol* **2007**, *4*, 255–258.
12. Bersani, D.; Salvioli-Mariani, E.; Mattioli, M.; Menichetti, M.; Lottici, P. Raman and micro-thermometric investigation of the fluid inclusions in quartz in a gold-rich formation from Lepaguare mining district (Honduras, Central America). *Spectrochim. Acta Part A Mol. Biomol. Spectrosc.* **2009**, *73*, 443–449. [CrossRef]
13. Mattioli, M.; Menichetti, M.; Renzulli, A.; Toscani, L.; Salvioli-Mariani, E.; Suarez, P.; Murroni, A. Genesis of the hydrothermal gold deposits in the Canan area, Lepaguare District, Honduras. *Int. J. Earth Sci.* **2014**, *103*, 901–928. [CrossRef]
14. Nelson, C. *Metallic Mineral Resources*; Taylor & Francis: Milton Park, UK, 2006; Volume 158, pp. 885–915.
15. AID. *Honduras Recursos Minerales L11 [Honduras Mineral Resources L11], 1 Sheet, Scale 1:1,000,000*; Technical Report; U.S. Army Corps of Engineers: Washington, DC, USA, 1965.
16. Marco, C.R. *Geologico Del Mapa Metalogenetico De Honduras*; Technical Report; MDC Honduras: Tegucigalpa, Honduras, 2011.
17. Fairbrother, L.; Brugger, J.; Shapter, J.; Laird, J.S.; Southam, G.; Reith, F. Supergene gold transformation: Biogenic secondary and nano-particulate gold from arid Australia. *Chem. Geol.* **2012**, *320*, 17–31. [CrossRef]
18. Knight, J.; Morison, S.; Mortensen, J. The relationship between placer gold particle shape, rimming, and distance of fluvial transport as exemplified by gold from the Klondike District, Yukon Territory, Canada. *Econ. Geol.* **1999**, *94*, 635–648. [CrossRef]
19. Hough, R.M.; Butt, C.R.; Fischer-Bühner, J. The crystallography, metallography and composition of gold. *Elements* **2009**, *5*, 297–302. [CrossRef]
20. Masson, F.X.; Beaudoin, G.; Laurendeau, D. Multi-method 2D and 3D reconstruction of gold grain morphology in alluvial deposits: A review and application to the Rivière du Moulin (Québec, Canada). *Geol. Soc. Lond. Spec. Publ.* **2022**, *516*, 337–352. [CrossRef]
21. Townley, B.K.; Hérail, G.; Maksaev, V.; Palacios, C.; Parseval, P.d.; Sepulveda, F.; Orellana, R.; Rivas, P.; Ulloa, C. Gold grain morphology and composition as an exploration tool: Application to gold exploration in covered areas. *Geochem. Explor. Environ. Anal.* **2003**, *3*, 29–38. [CrossRef]

22. Pindell, J.L. Evolution of the Gulf of Mexico and the Caribbean. In *Caribbean Geology: An Introduction*; The University of the West Indies Press: Kingston, Jamaica, 1994; pp. 13–39.
23. Rogers, R.D.; Mann, P. Transtensional deformation of the western Caribbean-North America plate boundary zone. *Spec.-Pap.-Geol. Soc. Am.* **2007**, *428*, 37.
24. Corti, G.; Carminati, E.; Mazzarini, F.; Garcia, M.O. Active strike-slip faulting in El Salvador, central America. *Geology* **2005**, *33*, 989–992. [CrossRef]
25. Rogers, R.D.; Mann, P.; Emmet, P.A. Tectonic terranes of the Chortis block based on integration of regional aeromagnetic and geologic data. *Spec.-Pap.-Geol. Soc. Am.* **2007**, *428*, 65.
26. Salvioli-Mariani, E.; Toscani, L.; Boschetti, T.; Bersani, D.; Mattioli, M. Gold mineralisations in the Canan area, Lepaguare District, east-central Honduras: Fluid inclusions and geochemical constraints on gold deposition. *J. Geochem. Explor.* **2015**, *158*, 243–256. [CrossRef]
27. Nazzareni, S.; Comodi, P.; Bindi, L.; Safonov, O.G.; Litvin, Y.A.; Perchuk, L.L. Synthetic hypersilicic Cl-bearing mica in the phlogopite-celadonite join: A multimethodical characterization of the missing link between di-and tri-octahedral micas at high pressures. *Am. Mineral.* **2008**, *93*, 1429–1436. [CrossRef]
28. Schindelin, J.; Rueden, C.T.; Hiner, M.C.; Eliceiri, K.W. The ImageJ ecosystem: An open platform for biomedical image analysis. *Mol. Reprod. Dev.* **2015**, *82*, 518–529. [CrossRef]
29. Alunno, S.; Nazzareni, S.; Luca, B.; Mattioli, M.; Renzulli, A.; Menichetti, M. Is ethical gold possible? The example from fluvial gold placer in Lepaguare mining district (Honduras, Central America). In *Proceedings of the Mineral Deposit Research for A High-Tech World*; Jonsson, E., Ed.; Uppsala Univ; Stockholm Univ; Lulea Univ Technol; Geol Survey Finland & Norway; Swedish Museum Nat Hist; Boliden AB; LKAB; Agnico-Eagle Mines Ltd; Mawson Resources Ltd; IMA-COM; CODMUR/IAGOD; IGCP/SIDA; SEG: Houston, TX, USA, 2013; Volume 1–4. pp. 292–293.
30. Chapman, R.J.; Banks, D.A.; Styles, M.T.; Walshaw, R.D.; Piazolo, S.; Morgan, D.J.; Grimshaw, M.R.; Spence-Jones, C.P.; Matthews, T.J.; Borovinskaya, O. Chemical and physical heterogeneity within native gold: Implications for the design of gold particle studies. *Miner. Depos.* **2021**, *56*, 1563–1588. [CrossRef]
31. Chapman, R.J.; Moles, N.R.; Bluemel, B.; Walshaw, R.D. Detrital gold as an indicator mineral. *Geol. Soc. Lond. Spec. Publ.* **2022**, *516*, 313–336. [CrossRef]
32. Chapman, R.J.; Craw, D.; Moles, N.R.; Banks, D.A.; Grimshaw, M.R. Evaluation of the contributions of gold derived from hypogene, supergene and surficial processes in the formation of placer gold deposits. *Geol. Soc. Lond. Spec. Publ.* **2022**, *516*, 291–311. [CrossRef]
33. Potter, M.; Styles, M. Gold characterisation as a guide to bedrock sources for the Estero Hondo alluvial gold mine, western Ecuador. *Appl. Earth Sci.* **2003**, *112*, 297–304. [CrossRef]